Investigation of fusion probabilities in the reactions with ^{52,54}Cr, ^{64}Ni, and ^{68}Zn ions leading to the formation of $Z = 120$ superheavy composite systems

K. V. Novikov,[1] E. M. Kozulin,[1] G. N. Knyazheva,[1] I. M. Itkis ◉,[1] M. G. Itkis,[1] A. A. Bogachev,[1] I. N. Diatlov,[1] M. Cheralu,[1]
D. Kumar,[1] N. I. Kozulina,[1] A. N. Pan,[1,2] I. V. Pchelintsev,[1] I. V. Vorobiev,[1] W. H. Trzaska,[3] S. Heinz,[4] H. M. Devaraja,[4]
B. Lommel,[4] E. Vardaci,[5,6] S. Spinosa,[5,6] A. Di Nitto,[5,6] A. Pulcini,[5,6] S. V. Khlebnikov,[7] Pushpendra P. Singh,[8]
Rudra N. Sahoo,[8] B. Gall,[9] Z. Asfari,[9] C. Borcea,[10] I. Harca,[10] and D. M. Filipescu[10]

[1]*Flerov Laboratory of Nuclear Reactions, Joint Institute for Nuclear Research, 141980 Dubna, Russia*
[2]*Laboratory of Fission Physics, Institute of Nuclear Physics, Almaty, 480082 Kazakhstan*
[3]*Department of Physics, University of Jyväskylä, FIN-40014 Jyväskylä, Finland*
[4]*GSI Helmholtzzentrum für Schwerionenforschung, 64291 Darmstadt, Germany*
[5]*Dipartimento di Fisica "E. Pancini," Universita degli Studi di Napoli "Federico II," 80126 Napoli, Italy*
[6]*Istituto Nazionale di Fisica Nucleare, Sezione di Napoli, 80126 Napoli, Italy*
[7]*Khlopin Radium Institute, St. Petersburg, Russia*
[8]*Department of Physics, Indian Institute of Technology Ropar, Rupnagar, Punjab 140001, India*
[9]*Hubert Curien Multidisciplinary Institute, University of Strasbourg, Strasbourg, 67037 France*
[10]*Horia Hulubei National Institute for Physics and Nuclear Engineering, 077125 Bucharest-Măgurele, Romania*

Background: The formation of superheavy nuclei in fusion reactions is suppressed by a competing quasifission process. The competition between the formation of the compound nucleus and the quasifission depends strongly on the reaction entrance channel.

Purpose: The investigation of fission and quasifission processes in the formation of $Z = 120$ superheavy composite systems in the ^{52,54}Cr + ^{248}Cm and ^{68}Zn + ^{232}Th reactions, and their comparison with the ^{64}Ni + ^{238}U reaction at energies in the vicinity of the Coulomb barrier.

Methods: Mass-energy distributions of fissionlike fragments formed in the reactions ^{52,54}Cr + ^{248}Cm and ^{68}Zn + ^{232}Th at energies near the Coulomb barrier were measured using the double-arm time-of-flight spectrometer CORSET.

Results: Capture cross sections for the reactions under investigation were measured. The most probable fragment masses and total kinetic energies as well as their variances in dependence on the interaction energy were studied for asymmetric and symmetric fragments. The fusion probabilities were estimated from the analysis of mass-energy distributions.

Conclusions: The estimated fusion probability drops down by a factor of 10^3 in the ^{54}Cr + ^{248}Cm reaction compared to the reactions of ^{48}Ca ions with actinides. Among the studied reactions, the ^{54}Cr + ^{248}Cm is the most favorable one for the production of the superheavy element with $Z = 120$.

I. INTRODUCTION

The extension of the upper part of the nuclide chart is one of the major goals of modern superheavy element physics. The heaviest element known today is Oganesson (^{294}Og) with $Z = 118$. Nuclei of the element were produced in the complete fusion reaction of ^{48}Ca ions with ^{249}Cf [1]. According to theoretical predictions, the "island of stability" is expected near the neutron shell at $N = 184$ and proton shells at $Z = 114$ or $Z = 120-126$ [2,3]. The proton closed shell number has not yet been established unequivocally since theoretical models give different predictions and strongly depend on the choice of the parameters for nucleon-nucleon interactions in the nucleus. The available experimental data have not yet allowed defining these numbers. Therefore, the production

of superheavy elements with $Z > 118$ and the investigation of their properties is of particular interest in studying the island of stability. Unfortunately, superheavy nuclei (SHN) formed in ^{48}Ca-induced reactions cannot reach the predicted neutron closed shell with $N = 184$ due to the lack of seven to nine neutrons. To go beyond $Z = 118$, projectiles heavier than ^{48}Ca must be applied because necessary target materials are lacking. However, at the transition to the heavier projectiles, an increase in the Coulomb repulsion between the interacting nuclei gives rise to quasifission (QF) and deep inelastic processes, which strongly suppress the formation of the compound nucleus (CN).

QF [4–7] and deep inelastic collisions (DICs) [8] are considered binary multinucleon transfer reactions with a full momentum transfer in which the composite system separates

TABLE I. The entrance channel properties for the reactions leading to the formation of the $Z = 120$ superheavy composite system. $Z_1 Z_2$ is the Coulomb factor, x_{eff} is the effective fissility parameter [19], x_m is the mean fissility parameter [20], and $\alpha_0 = (A_t - A_p)/(A_t + A_p)$ is the entrance channel mass asymmetry.

Reaction	System	$Z_1 Z_2$	x_{eff}	x_m	α_0	Reference
^{50}Ti + ^{249}Cf	^{299}120	2156	0.788	0.845	0.666	[24]
^{52}Cr + ^{248}Cm	^{300}120	2304	0.830	0.877	0.653	This paper
^{54}Cr + ^{248}Cm	^{302}120	2304	0.820	0.868	0.642	This paper, [24]
^{58}Fe + ^{242}Pu	^{300}120	2444	0.849	0.890	0.616	[14]
^{64}Ni + ^{238}U	^{302}120	2576	0.866	0.903	0.576	[14,24]
^{68}Zn + ^{232}Th	^{300}120	2700	0.891	0.922	0.547	This paper
^{95}Rb + ^{209}Bi	^{304}120	3071	0.922	0.944	0.375	[25]

after the capture in two main fragments without forming a CN and characterized by sufficient energy dissipation and mass transfer. There is no clear separation between QF and DICs processes. Typically, the angular distributions of DICs are mainly focused near the grazing angles of collisions, DIC evolution time being a few zeptoseconds. Mass distributions are peaked around the projectile and target nuclei masses, and the yield of fragments with masses heavier or lighter than interacting nuclei decreases exponentially. QF is characterized by smoother angular distributions, and its evolution time can extend up to tens of zeptoseconds. As a rule, shell effects have a significant impact on the yield of QF fragments, leading to the asymmetric mass distributions with heavy fragment peak near the mass $A = 208$ ($Z = 82$ and/or $N = 126$) for heavy-ion reactions leading to the formation of superheavy systems.

Current theoretical calculations used to describe the evolution of low-energy nucleus-nucleus collisions with strong channel coupling leading to CN formation, DIC, and QF [9–13] show that QF can be of two types. The first type of QF (the so-called asymmetric QF) associated with fast reaction times (a few zeptoseconds) is characterized by asymmetric angular distributions in the center-of-mass (c.m.) system and a wide double-hump mass distribution with mass asymmetry ≈ 0.4. The second type of QF (the so-called symmetric QF) is a rather slow process, comparable with CN fission, leading to the formation of symmetric fragments and characterized by symmetric angular distributions. Since both CN fission and symmetric QF have similar mass and angular distributions, drawing a clear distinction between the two processes is extremely difficult. Nevertheless, it is only CN fission that passes through a true saddle point. Therefore, the difference in shape evolution and energy dissipation for CN fission and symmetric QF may lead to different total kinetic energy (TKE) distributions for the processes.

The evaluation of the CN fission contribution to all fission-like fragments based on the analysis of the TKE distribution of symmetric fragments formed in heavy-ion-induced reactions was applied in Refs. [14–18]. This approach allows the experimental estimation of the upper limit of the fusion probability P_{CN}.

SHN with $Z = 120$ and $N = 180$–182 may be produced in complete fusion reactions of ^{50}Ti, ^{54}Cr, ^{58}Fe, ^{64}Ni, and ^{68}Zn ions with actinide target nuclei. The reaction entrance channel properties are presented in Table I. Larger reaction

parameters, such as the Coulomb factor $Z_1 Z_2$, effective [19], and mean fissilities [20] as compared to those of the Ca-induced reactions are expected to significantly increase the contribution of QF to the capture cross section for the reactions. Attempts to synthesize superheavy element with $Z = 120$ using the ^{58}Fe beam in Dubna [21] and the ^{64}Ni beam in Darmstadt [22] were unsuccessful. Beams of ^{50}Ti and ^{54}Cr are considered to be an alternative option. In an attempt to produce the element at GSI [23] in the ^{54}Cr + ^{248}Cm reaction, a possibility of assigning the observed decay sequence to the isotope of element 120 was discussed. However, the results could not be confirmed by the existing experimental data. The experimentally defined P_{CN} can contribute to understanding the underlying reaction mechanisms. The ^{50}Ti + $^{249-251}$Cf reaction is supposed to have the highest fusion probability, but the production of an intense Ti beam, unlike Cr beams, involves a fair number of difficulties due to the physicochemical properties of Ti.

In this paper, the mass and energy distributions of binary fragments formed in the ^{52,54}Cr + ^{248}Cm and ^{68}Zn + ^{232}Th reactions leading to the composite system with $Z = 120$ at energies near the Coulomb barrier were measured and compared with those of the ^{64}Ni + ^{238}U reaction [14]. The analysis aimed at estimating the fusion probability at the transition from the reactions with Cr ions to the ^{64}Ni- and ^{68}Zn-induced reactions. In addition, a possibility of producing the CN with $Z = 120$ and $N = 184$ in the fusion reaction of radioactive Rb beams and the ^{209}Bi target is discussed.

II. EXPERIMENT

The experiments were performed using the U400 cyclotron at the Flerov Laboratory of Nuclear Reactions (FLNR), Dubna, Russia, and K-130 cyclotron at the Physics Department of the Jyväskylä University, Finland. At FLNR a 200-μg/cm^2 ^{248}Cm target deposited as oxides onto a 1.3-μm titanium backing was irradiated with the 290- and 304-MeV ^{52}Cr and 296-MeV ^{54}Cr beams. In Jyväskylä, the reactions ^{64}Ni + ^{238}U and ^{68}Zn + ^{232}Th were investigated. The 355-MeV ^{68}Zn beam bombarded a thorium target prepared by evaporating ^{232}ThF$_4$ (250 μg/cm^2) on 35-μg/cm^2 carbon backing. The details of measurements for the reaction ^{64}Ni + ^{238}U were described in Ref. [14]. In experiments, the target backings faced the beam. The energy resolution was
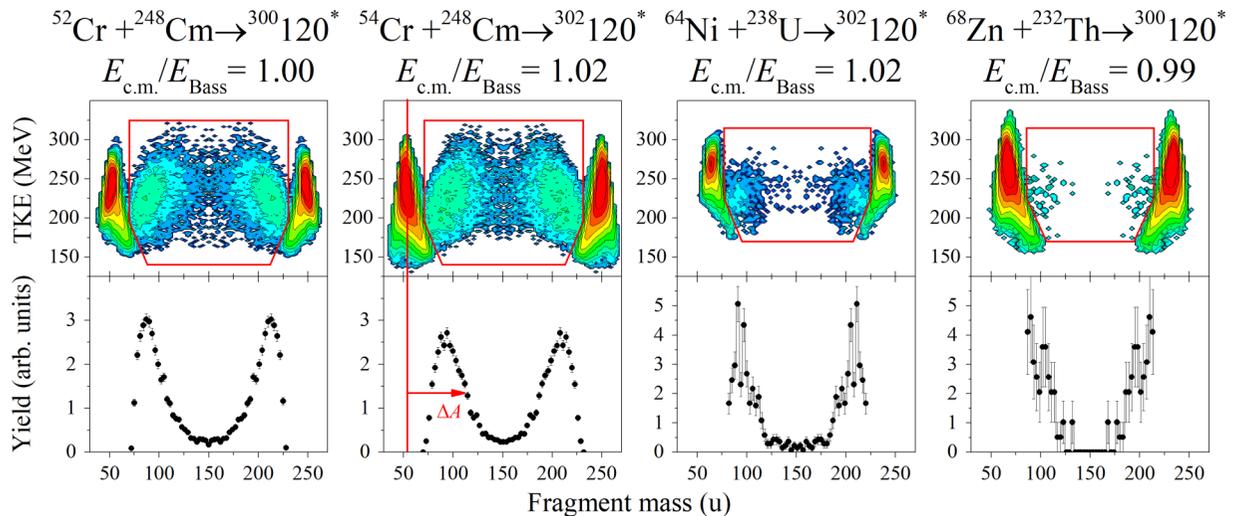
FIG. 1. The mass and energy distributions of binary fragments formed in the reactions ^{52,54}Cr + ^{248}Cm, ^{64}Ni + ^{238}U, and ^{68}Zn + ^{232}Th leading to the formation of composite systems with $Z = 120$ at energies near the Coulomb barrier. Top panels: M-TKE matrices of binary reaction products. Bottom panels: mass distributions of fissionlike fragments inside the polygons in M-TKE matrices.

about 1%. Beam intensities on targets were 1 to 2 pnA. The enrichment of the targets was 99.99%.

The binary reaction products were measured in coincidence by the double-arm time-of-flight spectrometer CORSET [26]. Each arm of the spectrometer consists of a compact start detector and a position-sensitive stop detector based on microchannel plates. The angular acceptance of the spectrometer in the reaction plane was $\pm 14°$. In the experiments, the main attention was paid to the measurement of symmetric fragments formed in the complete fusion reactions. According to the kinematics of the symmetric reaction fragments, the spectrometer arms were, thus, positioned at the symmetrical angles corresponding to 90° in the center-of-mass system. The position resolution of the stop detectors was 0.3°, and the time resolution was about 150 ps. The mass and energy resolutions of the CORSET setup were deduced from the full width at half maximum of the mass and energy spectra of elastic particles, respectively. The mass and TKE resolution of the spectrometer under these conditions was ± 2 u and ± 10 MeV, respectively.

Data processing assumed standard two-body kinematics [15]. Primary masses, velocities, energies, and angles of reaction products in the center-of-mass system were calculated from the measured velocities and angles using the momentum and mass conservation laws, assuming that the mass of the composite system is equal to $M_{\text{target}} + M_{\text{projectile}}$. Corrections for fragment energy losses in the target material and the foils of detectors were taken into account. The extraction of the binary reaction channels exhibiting full momentum transfer was based on the analysis of the kinematical diagram (see Refs. [15,27] for details).

III. RESULTS AND DISCUSSION

The mass-total kinetic energy (M-TKE) distributions of primary binary fragments obtained in the ^{52,54}Cr + ^{248}Cm, ^{64}Ni + ^{238}U, and ^{68}Zn + ^{232}Th reactions at energies close to

the Coulomb barrier are shown in Fig. 1. All the reactions lead to the formation of composite systems with $Z = 120$. In the M-TKE distributions, the reaction products with masses close to those of the projectile and target having energies around $E_{\text{c.m.}}$ were associated with elastic and quasielastic events and could be separated well enough from other reaction channels. The measurements were performed at correlation angles lower than the grazing angle; therefore, the contribution of DIC events to the experimental M-TKE distributions is insignificant. Fissionlike products located between the quasielastic peaks within the polygons in the M-TKE distributions (see Fig. 1) are characterized by large mass transfer and energy dissipation and can originate either from CN-fission or QF processes. The mass distributions of these events (inside the polygons of the M-TKE distributions) are presented in the bottom panels of Fig. 1.

The mass-energy distributions for the reactions with ^{52,54}Cr are similar to those of the reactions of ^{48}Ca with actinide target nuclei [16]. The pronounced asymmetric QF component with heavy fragments in the vicinity of the double magic lead is clearly observed. The mass distributions for the ^{64}Ni- and ^{68}Zn-induced reactions are also asymmetric, the most probable heavy QF fragments mass being 210–212 u for ^{64}Ni + ^{238}U. However, the QF peaks are notably narrower as compared to those of the ^{52,54}Cr + ^{248}Cm reactions. For the ^{68}Zn-induced reaction, QF overlaps with quasielastic events even stronger, and the heavy QF fragments peak is shifted towards more asymmetric masses. The drift of asymmetric QF toward mass symmetry (ΔA) estimated as a difference between the projectile mass and a more symmetric mass at half-maximum yield of QF (A_{HM}) decreases from 58 u for the reaction with ^{54}Cr, 54 u for ^{52}Cr, 38 u for ^{64}Ni to 29 u for the ^{68}Zn-induced reaction.

The analysis of experimental mass and angular distribution of fissionlike fragments formed in the reactions with ^{238}U ions showed [4] that the mass drift toward symmetry exhibited the properties of an overdamped motion with a universal
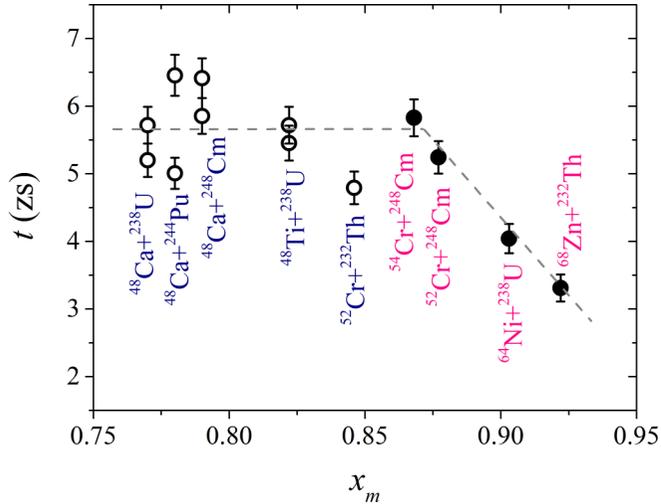
FIG. 2. The estimated time for asymmetric QF processes for the studied reactions (solid circles) in comparison with those obtained for the reactions of ^{48}Ca and ^{48}Ti ions with actinide nuclei (open circles) as a function of the mean fissility parameter. The dashed lines guide the eye.

FIG. 3. The capture cross section (solid circles) for the reactions ^{52,54}Cr + ^{248}Cm, ^{64}Ni + ^{238}U [14], and ^{68}Zn + ^{232}Th at energies $E_{c.m.}/E_{Bass} = 1.00$–1.02 in comparison with capture cross section (open circles) for the reactions of ^{26}Mg, ^{36}S, ^{48}Ca, and ^{48}Ti with actinide nuclei [15–17] and ^{48}Ca + ^{208}Pb [29] as a function of the effective fissility parameter. The dashed lines guide the eye.

time constant independent of scattering system and bombarding energy. We estimated the mean reaction time for the asymmetric QF process from the mass drifts for the studied systems using the relation between the mass drift and mean reaction time proposed in Ref. [4],

$$\frac{\Delta A}{\Delta A_{\max}} = \frac{A_{\mathrm{HM}} - A_p}{\frac{1}{2}(A_t - A_p)} = 1 - \exp\left[-(t - t_0)/\tau\right],$$

where A_p and A_t are the projectile and target masses, $\tau = (5.3 \pm 1)$ zs is the time constant common to all systems, $t_0 \approx 1$ zs is a time delay before mass drift sets in. Figure 2 shows the comparison of the estimated asymmetric QF times for the reactions under consideration and those for the reactions of ^{48}Ca [16] and ^{48}Ti [18] ions with actinide target nuclei at energies near the Coulomb barrier in dependence on mean fissility parameter. The mean fissility parameter $x_m = 0.25x_{\mathrm{CN}} + 0.75x_{\mathrm{eff}}$ has been recently proposed in Ref. [20] as a possible criterion for identifying the reaction mechanism. It is defined as a linear combination between the fissility parameter of the compound nucleus x_{CN}, reflecting the ratio of the competing repulsive Coulomb and attractive nuclear forces, and the effective fissility parameter x_{eff}, which takes account of the effect of the entrance channel mass and charge asymmetry.

It is clearly seen from Fig. 2 that the reaction time for asymmetric QF process barely changes in the ^{48}Ca-, ^{48}Ti-, and ^{52,54}Cr-induced reactions and is about 5–7 zs. However, it decreases at the transition to the reactions with ^{64}Ni and ^{68}Zn ions and amounts to 4 and 3 zs, respectively. The decrease in the reaction time for such systems is due to the strong Coulomb repulsion between interacting nuclei, which leads to the rather quick decay of the formed dinuclear system. It is to be noted that the values are in good agreement, although slightly exceed those obtained from the measured mass and angular distributions of the reaction fragments in Ref. [24]. In
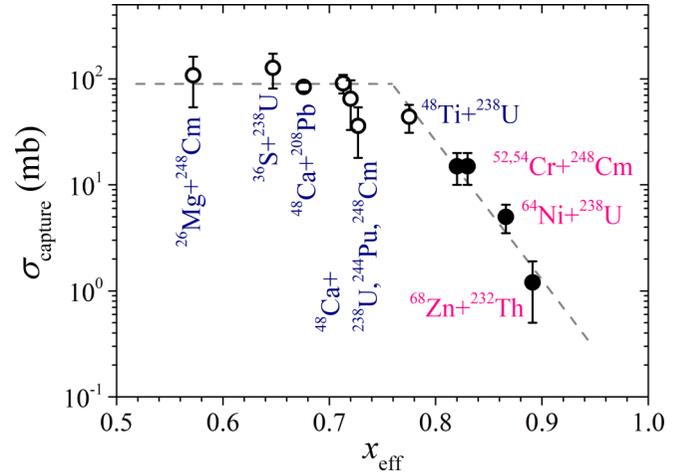
our study, the fragments with fast decay times were cut out due to the angular arrangement of the spectrometer arms, whereas a wider angular coverage of the setup used in Ref. [24] allowed the measurement of reaction fragments with shorter contact times. However, the formation of long-lived dinuclear systems does not necessarily indicate the formation of a CN. For instance, signatures for the formation of long-lived dinuclear systems were observed in the ^{64}Ni + ^{207}Pb, ^{132}Xe + ^{208}Pb, and ^{238}U + ^{238}U reactions measured at the velocity filter SHIP at the GSI and VAMOS spectrometer at GANIL [28], but the formation of CN was not expected for these systems.

Experimentally, the capture cross section is defined as a sum of the QF, CN fission, and evaporation residue cross sections. The absolute differential cross sections for all fissionlike events observed in the reactions ^{52,54}Cr + ^{248}Cm and ^{68}Zn + ^{232}Th were measured at the angle $\vartheta_{c.m.} \approx 90°$ and at energies near the Coulomb barrier. As mentioned previously, these angles are favorable for the registration of reaction fragments originated from CN-fission process. Since the angular coverage of the spectrometer is about 30°, the capture cross sections $\sigma_{\mathrm{capture}}$ for all fissionlike events were estimated assuming that the angular distribution is proportional to $1/\sin\vartheta_{c.m.}$.

In Fig. 3, the measured capture cross sections as a function of the effective fissility parameter x_{eff} are shown together with the data obtained for the reactions ^{48}Ca + ^{208}Pb [29] and the reactions of ^{26}Mg, ^{36}S, ^{48}Ca, ^{48}Ti [15–17] with actinide nuclei at interaction energies near the Coulomb barrier. For $x_{\mathrm{eff}} < 0.75$, the capture cross sections hardly change at all. For x_{eff} larger than 0.75, the capture cross sections decrease exponentially with increasing effective fissility parameter. In this case, the main reaction channel is a few-nucleon transfer process. For example, for the ^{64}Ni + ^{238}U reaction at the energy 13% above the barrier, the capture cross section is lower than the
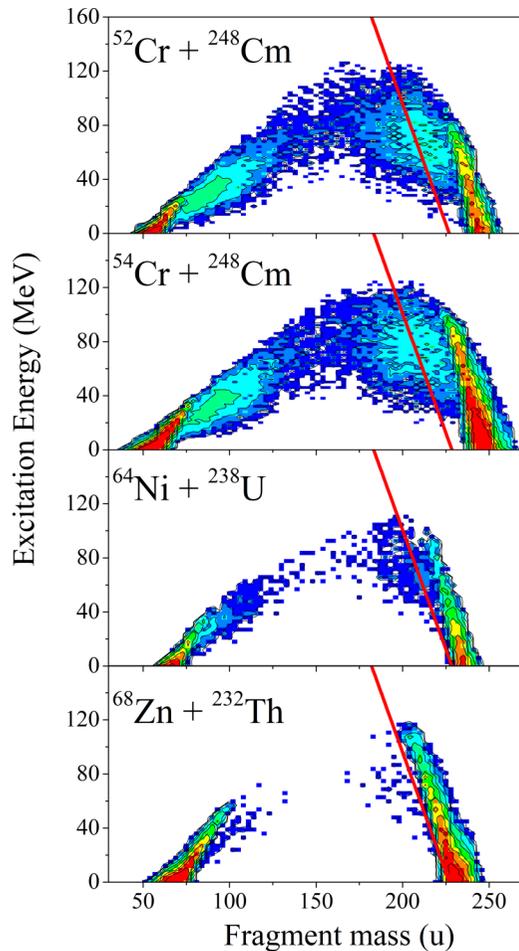
FIG. 4. Excitation energy of primary fragments formed in the ^{52,54}Cr + ^{248}Cm, ^{64}Ni + ^{238}U, and ^{68}Zn + ^{232}Th reactions at energies near the Coulomb barrier as a function of mass. The solid lines correspond to the estimated excitation energy of the fragments where $\Gamma_n = \Gamma_f$ and separate the reaction fragments into the domains of deexcitation by neutron emission and fission, respectively (see the text for an explanation).

total transfer cross section measured in Ref. [30] by a factor of 5.5. In the case of the ^{68}Zn + ^{232}Th reaction, the capture cross section decreases by about one order of magnitude compared to the cross sections for the reactions with $x_{\text{eff}} < 0.75$.

From the measured mass-energy distributions of the reaction fragments of the studied nuclear systems, the available excitation energy of both fragments expressed by $E_f^* = E_{\text{c.m.}} - \text{TKE} + Q_{gg}$ was estimated under the assumption that the excitation was divided between two primary fragments in proportion to their masses [31]. The distributions of obtained excitation energy for each fragment are shown in Fig. 4. The solid lines correspond to the case where the fission width Γ_f and the neutron width Γ_n are equal [32]. The influence of the fragment spin on the fission barrier was neglected. The condition $\Gamma_n = \Gamma_f$ in relation to the excitation energy of the formed fragments reflects the boundary between the regimes of deexcitation of the formed excited primary reaction fragments by neutron emission and fission. For fisssionlike fragments

with excitation energies higher than critical excitation (solid lines in Fig. 4), the sequential fission of heavy fragments is expected. As clearly seen in Fig. 4, the bulk of heavy fragments formed in the reactions with ^{52,54}Cr ions have excitation energies higher than the estimated critical excitation. Since in the double velocities measurement method both fragments have to be detected in coincidence, and, therefore, the events will be lost in the case of deexcitation of fragments via fission, the sequential fission of heavy fragments due to their relatively high excitation energy may result in the decrement of the capture cross section.

But in the case of the reactions with ^{64}Ni and, particularly, ^{68}Zn ions the excitation of most fissionlike fragments is lower than the critical value, thus, the both reaction fragments are expected to survive during the deexcitation process. Therefore, DIC is a dominant channel for these reactions and most fissionlike fragments are focused near the angles of grazing collisions, so they were not detected in experiments due to the angular acceptance of the CORSET spectrometer. It is to be noted that according to the calculations within the macroscopic-microscopic model of Swiatecki [33], the Z_1Z_2 threshold value for the appearance of QF is 1600 and for $Z_1Z_2 \geqslant 2600$ the main reaction mechanism is DIC. Consequently, we may expect a decrease in the QF contribution to the capture cross section for the reactions with ^{64}Ni ($Z_1Z_2 = 2576$) and particularly with ^{68}Zn ($Z_1Z_2 = 2700$) ions.

Since the formation of symmetric fragments is a rather slow process even in the case of QF, a decrease in the dinuclear system lifetime results in the reduction of their production cross section. To form these fragments, a composite system should exist more than 10^{-20} s [4,5], which is long enough for the formation of a compound nucleus. As a first step in evaluating the CN-fission cross section, the contribution of fragments with masses $A_{\text{CN}}/2 \pm 20$ u can be taken into consideration. For the systems with $Z = 108$–114, the CN-fission fragments mass distributions can have a symmetric Gaussian shape with the standard deviation of about 20 u (as in the case of Hs [15]) as predicted by the liquid drop model, or an asymmetric shape caused by the influence of the closed shells with $Z = 50$ and $N = 82$ as in the case of fission of actinides [34]. In both cases, the width of the mass distributions of the CN-fission fragments does not exceed 40 u. Therefore, the choice of the mass range of $A_{\text{CN}}/2 \pm 20$ u is reasonable.

Figure 5 shows the contributions of symmetric fragments to the capture cross section for the ^{52,54}Cr + ^{248}Cm, ^{64}Ni + ^{238}U reactions, and their dependence on interaction energy. In the case of the ^{68}Zn + ^{232}Th reaction, no symmetric fragments were observed within the mass range of $A_{\text{CN}}/2 \pm 20$ u. The yield of symmetric fragments formed in the reaction ^{48}Ca + ^{238}U leading to the formation of a composite system with $Z = 112$ is shown for comparison since this reaction was comprehensively studied in Refs. [4,16,35]. As can clearly be seen from Fig. 5, the contribution of symmetric fragments in the case of the ^{48}Ca + ^{238}U reaction monotonically increases with increasing interaction energy, whereas the growth is very slow in the case of the ^{52}Cr + ^{248}Cm and ^{64}Ni + ^{238}U reactions.

Figure 6 shows the contributions of symmetric fragments to the capture cross section as a function of the mean
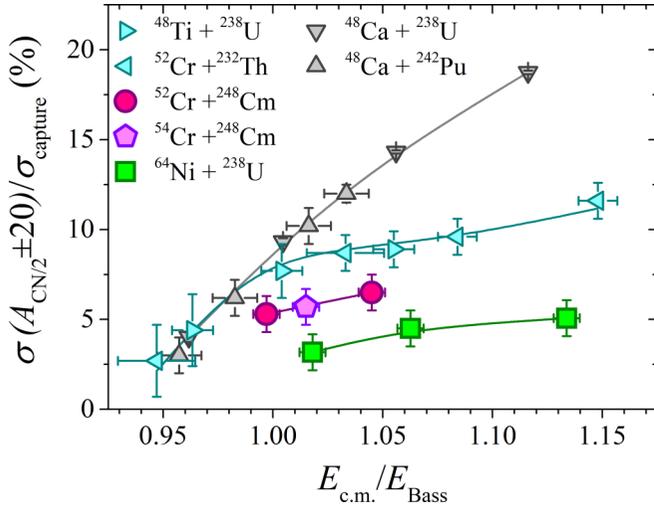
FIG. 5. Contributions of the symmetric fragments to the capture cross sections as a function of energy above the barrier for the studied systems in comparison with the reactions ^{48}Ca + ^{238}U, ^{244}Pu, ^{48}Ti + ^{238}U, and ^{52}Cr + ^{232}Th [18].

fissility parameter x_m for the ^{52,54}Cr + ^{248}Cm, ^{64}Ni + ^{238}U, ^{48}Ca + ^{238}U, ^{48}Ca + ^{244}Pu, ^{48}Ti + ^{238}U, ^{52}Cr + ^{232}Th, and ^{86}Kr + ^{198}Pt reactions [18] at energies near the Coulomb barrier. It should be noted that in the case of the ^{48}Ti + ^{238}U, ^{52}Cr + ^{232}Th, and ^{86}Kr + ^{198}Pt reactions with $Z_1 Z_2 > 2000$ [18] the yield of symmetric fragments grows slowly with increasing interaction energy as in the case of the ^{52}Cr + ^{248}Cm and ^{64}Ni + ^{238}U reactions, whereas in the case of reactions with $Z_1 Z_2 < 2000$ the contribution of symmetric fragments is similar to that of the ^{48}Ca + ^{238}U reaction. As can be seen from Fig. 6, the yield of symmetric fragments decreases with
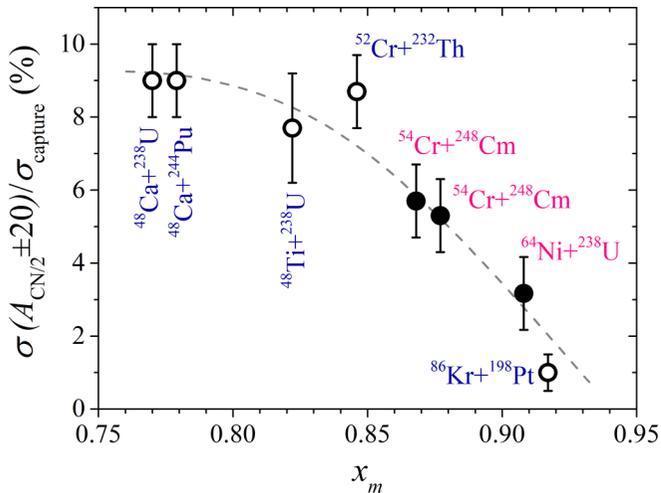

FIG. 6. Contributions of symmetric fragments to the capture cross section for the studied systems (solid circles) as a function of the mean fissility parameter for the reactions ^{52,54}Cr + ^{248}Cm and ^{64}Ni + ^{238}U [14] at $E_{c.m.}/E_{Bass} = 1.00$–1.02 in comparison with the ^{48}Ca + ^{238}U, ^{244}Pu, ^{48}Ti + ^{238}U, ^{52}Cr + ^{232}Th, and ^{86}Kr + ^{198}Pt reactions (open circles) [18]. The dashed line guides the eye.
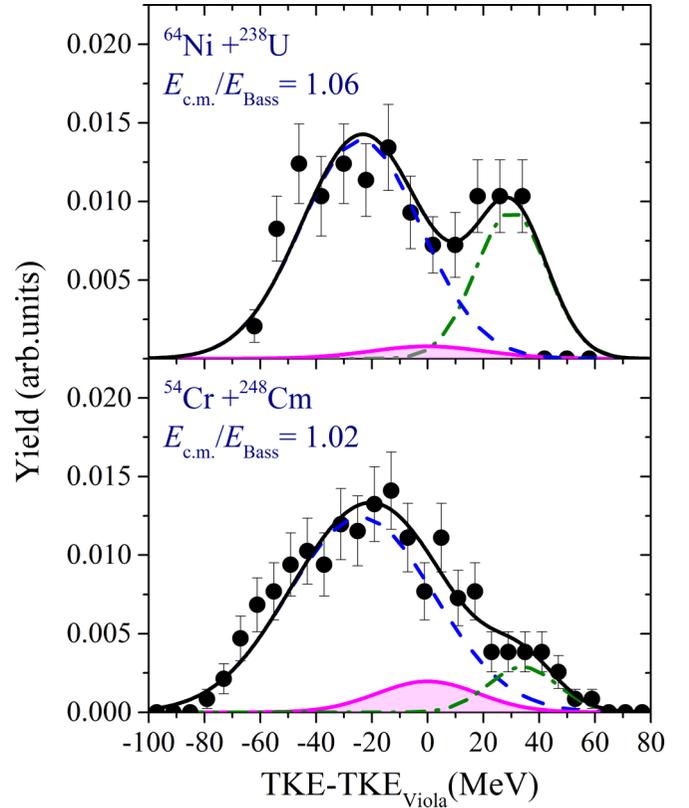

FIG. 7. TKE distributions of fragments with masses $A_{CN}/2 \pm 20$ u for the reactions ^{54}Cr + ^{248}Cm (bottom panel) and ^{64}Ni + ^{238}U (top panel) leading to the formation of the same composite system $Z = 120$ at energies above the Coulomb barrier. The filled region corresponds to the TKE distribution for CN fission for ^{54}Cr + ^{248}Cm. The dashed and dashed-dotted curves are associated with asymmetric and symmetric QF, respectively.

increasing x_m at energies near the Coulomb barrier. This may indicate a significant increase in the asymmetric QF process for the reactions with $Z_1 Z_2 > 2000$.

However, the symmetric fragments may be formed not only in CN-fission process, but also in slow nonequilibrium processes, such as symmetric or asymmetric QF or even DIC [36]. As mentioned above, the difference in descent to scission in CN fission and QF may affect the total kinetic energy of fragments. Therefore, the TKE distributions could give additional information on reaction dynamics. The analysis of a large set of experimental data on the fission process showed that the most probable TKE increased linearly with increasing CN fissility parameter $Z^2/A^{1/3}$ and could be well described by the Viola systematics [37]. The variance of TKE for the CN-fission process also increased and could be estimated using the systematics of Itkis and Rusanov [38].

The TKE distributions of symmetric fragments with masses $A_{CN}/2 \pm 20$ u for the ^{54}Cr + ^{248}Cm and ^{64}Ni + ^{238}U reactions are shown in Fig. 7. It is clearly seen that the TKE distributions differ markedly demonstrating a nearly Gaussian shape in the case of the ^{54}Cr + ^{248}Cm reaction and a two-humped shape for ^{64}Ni + ^{238}U. In contrast to the ^{48}Ca + ^{238}U

reaction [14,16,17] where the most probable TKE was close to the value of the Viola systematics (as expected for the CN fission), the maxima of TKE distributions for the $^{54}Cr + ^{248}Cm$ and $^{64}Ni + ^{238}U$ reactions are shifted towards lower energies.

We assume that the mass-symmetric fragments may be formed by three different modes: CN fission, symmetric QF, and a tail of the asymmetric QF process. Similar to modal fission caused by the valley structure of the potential surface of a fissile nucleus where each mode has its specific mass and energy distribution [34,39–42], we may expect different TKE distributions for asymmetric and symmetric QF processes.

To evaluate the contribution of the CN-fission process in the symmetric mass region, the TKE distributions were decomposed as a sum of three Gaussians. One of them was associated with the CN-fission process (filled region in Fig. 7). We fixed the mean value and variance of this component to the values obtained from the systematics presented in Refs. [37,38], respectively. The low-energy component in Fig. 7 is attributed to asymmetric QF, whereas the high-energy one is connected with symmetric QF. Higher TKE for symmetric QF as compared to CN fission may be caused by the stronger influence of the closed shells at $Z = 50$ and $N = 82$ on the QF process [43], whereas for asymmetric QF, which is driven by the lead double magic shell, lower TKE is expected due to the lower $Z_1 Z_2$ factor. In the fitting procedure, we also fixed the variance of the asymmetric QF component equal to the variance of TKE for the maximum yield of asymmetric QF.

P_{CN} is defined as the probability for CN formation from the configuration of two nuclei in contact. The cross section of the evaporation residues for SHN is negligibly small compared to the CN-fission cross section for these reactions. Thus, we can estimate the fusion probability using the measured mass-energy distributions as the ratio between the number of events attributed to CN fission within the scope of the present analysis and all fissionlike fragments. The estimated fusion probabilities for the studied reactions are shown in Fig. 8. Since no symmetric fragments were observed in the $^{68}Zn + ^{232}Th$ reaction, only the upper limit for P_{CN} could be obtained. Note that the target nuclei are well deformed in all the studied reactions. The dependence of fusion probability on the mean fissility parameter for hot fusion reactions with strongly deformed targets deduced from the analysis of mass-energy distributions in Ref. [17] is also shown in Fig. 8. The P_{CN} for the studied systems was obtained as a ratio between the yield of CN fission and the contact cross section, which is close to the geometrical one at above-barrier collision energies. Normalization to the contact cross section rather than the capture cross section allows one to avoid inaccuracies in the experimental capture cross section caused by the differentiation of fissionlike fragments from elastic/quasielastic events in mass-energy distributions of binary reaction fragments. Moreover, the procedure helps avoiding possible errors in integration of angular distributions for these fragments. The deduced P_{CN} values for the reactions $^{54}Cr + ^{248}Cm$ and $^{68}Zn + ^{232}Th$ are in good agreement with the description of P_{CN} using the equation from Ref. [17].
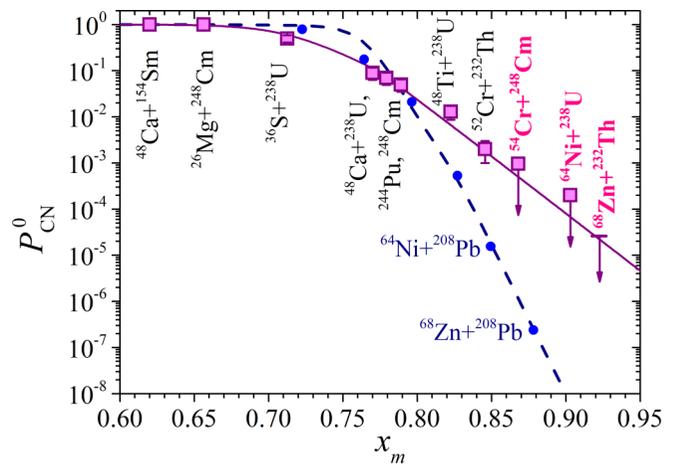

FIG. 8. Fusion probability for the $^{54}Cr + ^{248}Cm$ and $^{68}Zn + ^{232}Th$ reactions in comparison with fusion probabilities in hot fusion (with strongly deformed target nuclei) reactions [17] at energies above the Coulomb barrier as a function of the mean fissility parameter of the reaction. The circles denote the calculated fusion probabilities for cold fusion reactions [44].

Thus, based on the analysis of mass-energy distributions of symmetric reaction fragments, we estimated the fusion probabilities at energies above the Coulomb barrier: about 10^{-3} for $^{54}Cr + ^{248}Cm$, 10^{-4} for $^{64}Ni + ^{238}U$, and lower than 10^{-5} for $^{68}Zn + ^{232}Th$. Note that in the case of the involving ^{48}Ca ions and actinide nuclei, the fusion probabilities deduced with the same approach in Ref. [16] were about 10^{-1}. The excitation energies of CN formed in the fusion reactions of Ti, Cr, and Ni ions with actinide target nuclei are about 30–40 MeV at the Coulomb barrier energy that give a chance to observe $3n$ and $4n$ evaporation residue channels similar to the ^{48}Ca-induced reaction. Consequently, under the assumption of similar fission barriers for these SHN, the production cross section of SHN with $Z = 120$ using the $^{54}Cr + ^{248}Cm$ reaction is expected to be of about a few femtobarns. In the case of the $^{64}Ni + ^{238}U$ and $^{68}Zn + ^{232}Th$ reactions, the production cross sections are lower by one and two orders of magnitude, respectively.

Unfortunately, reactions with stable projectiles do not provide enough neutrons to reach the predicted neutron shell at $N = 184$ due to the bending of the stability line toward the neutron axis. After deexcitation (by evaporation of three to four neutrons), the number of neutrons in SHN formed in the studied reactions would be less than $N = 184$. However, SHN with $Z = 120$ and $N = 184$ may be formed in complete fusion reactions with neutron-rich radioactive ion beams (RIBs). The choice of the collision system is constrained by highly restricted suitable neutron-rich RIBs with sufficient intensity. To date RIBs with required energies (around 5 MeV/nucleon) are so far available at CERN's new HIE-ISOLDE facility. The highest beam intensities have been attained for heavy alkali metals and noble gases. Very neutron-rich ^{95}Rb beams hitting ^{209}Bi targets can be used to form SHN with $Z = 120$ and $N = 184$ [25]. In the case of complete fusion, the CN around $N = 184$ would be produced with excitation energies

$E^* < 5$ MeV at the Coulomb barrier. This excitation energy is half as low as that needed for the evaporation of one neutron and substantially lower than the predicted fission barrier $B_f \geqslant 7$ MeV. The CN would then be so cold as to make it impossible for neutrons to be evaporated.

For the exotic ^{95}Rb beam, one can expect 10^6–10^7 particles on the target. These intensities are still too low for observing fusion evaporation residues from this reaction. We can, therefore, expect only indirect information on the possible enhanced stability in the area $Z = 120$, $N = 184$ in the near and midterm future. We think that studying QF and CN-fission processes in the Rb + Bi compound systems might be a viable pathway. From a physics point of view, ^{95}Rb + ^{209}Bi is not an optimum combination because it is a "cold fusion system" with a relatively high entrance channel Coulomb barrier (Table I). According to the calculations of fusion probabilities for cold fusion reactions based on the analysis of evaporation residue cross sections by Zagrebaev and Greiner [44] (dotted line in Fig. 8), we can expect the fusion probability for this reaction of about 10^{-11}. However, these predictions were made for stable beams and SHN located far from the neutron shell at $N = 184$ (neutron deficit is more than 15 neutrons). Moreover, the ^{95}Rb nucleus is expected to have a neutron skin similar to ^{48}Ca nucleus ($r_n - r_p \approx 0.2$ fm) [45]. The neutron skin changes the balance between the nuclear and the Coulomb forces in the entrance channel and may lead to an increase in the fusion probability. Note that the heaviest SHN were produced in reactions with neutron-rich ^{48}Ca ions, and the study of QF and CN-fission processes in the ^{40,44,48}Ca + ^{204,208}Pb reactions [46] revealed a strong evidence of QF in the ^{40}Ca + ^{208}Pb reaction, whereas the smallest contribution of QF was found in the case of the ^{48}Ca + ^{208}Pb reaction, despite reaction partners being doubly magic for both systems. This effect may be caused by the neutron skin of ^{48}Ca ions. Thus, taking into account the shell structure of the formed CN and the potential neutron skin of ^{95}Rb, the fusion probability is expected to be higher than predicted for the cold fusion reactions. An experiment aimed at investigating fissionlike fragments formed in the reaction ^{95}Rb + ^{209}Bi could provide information on the formation of both the long-lived dinuclear composite system formed prior to the statistical equilibrium and a low-excited CN, if formed.

with ^{48}Ca ions with average reaction time of about 5–7 zs. Moreover, shorter reaction times of about 3 to 4 zs were observed in the case of Ni and Zn ions. From the comparison of mass and energy distributions and capture cross sections, it was found that the contribution of QF fragments formed in long-lived composite systems decreases sharply at the transition from systems with $Z_1 Z_2 \approx 2300$ (Cr ions) to those with $Z_1 Z_2 > 2500$ (Ni and particularly Zn ions). The main reaction channels are shown to be a few-nucleon transfer and DIC.

However, the properties of symmetric fragments change significantly at the transition from ^{48}Ca ions to ^{52,54}Cr ions. In the case of ^{64}Ni- and ^{68}Zn-induced reactions, these changes are drastic. The contribution of symmetric fragments to all fissionlike events is similar to the ^{48}Ti + ^{238}U reaction leading to the formation of the composite system with $Z = 114$. At energies above the barrier, the contribution does not undergo changes with increasing interaction energy and is about 5 to 6% for the reactions with ^{52}Cr ions, contrary to the reactions involving actinide nuclei and ^{48}Ca ions where the contribution of symmetric fragments increases monotonically. This may indicate a significant increase in the QF process at the transition from Ca to Ti and Cr ions. Thus, for the nuclear systems with $Z_1 Z_2 > 2000$, the quasifission is a dominant process even in the formation of symmetric fragments.

The fusion probabilities for the reactions ^{52,54}Cr + ^{248}Cm and ^{68}Zn + ^{232}Th were estimated on the basis of the analysis of mass and TKE distributions. The obtained fusion probabilities are in good agreement with the fusion probability dependence on the mean fissility parameter found for the reactions of well-deformed nuclei with ^{36}S, ^{48}Ca, ^{48}Ti, and ^{64}Ni ions. The fusion probability is found to drop by approximately three orders of magnitude at the transition from ^{48}Ca + ^{238}U to the ^{54}Cr + ^{248}Cm reaction and by more than a factor of 10^5 to the ^{68}Zn + ^{232}Th reaction at energies above the Coulomb barrier. Based on the obtained fusion probability for the ^{54}Cr + ^{248}Cm reaction, the production cross section of SHN with $Z = 120$ is expected to be about a few femtobarns. In the case of the ^{64}Ni + ^{238}U and ^{68}Zn + ^{232}Th reactions the production cross sections are one and two orders of magnitude lower, respectively.

IV. SUMMARY

To investigate the fusion probability in the reactions of ^{52,54}Cr and ^{68}Zn ions with actinide nuclei leading to the formation of the composite systems with $Z = 120$, the mass and energy distributions of binary fragments formed in the ^{52,54}Cr + ^{248}Cm and ^{68}Zn + ^{232}Th reactions were studied at energies around the Coulomb barrier and compared with the ^{64}Ni + ^{238}U reaction investigated previously. The measurements were performed in Dubna and in Jyväskylä using the double-arm time-of-flight spectrometer CORSET.

In the case of the reactions with Cr ions the properties of asymmetric QF fragments are similar to those of the reactions

[1] Y. T. Oganessian and V. K. Utyonkov, Nucl. Phys. **A944**, 62 (2015).

[2] A. Sobiczewski, F. A. Gareev, and B. N. Kalinkin, Phys. Lett. **22**, 500 (1966).

[3] K. Rutz, M. Bender, T. Bürvenich, T. Schilling, P.-G. Reinhard, J. A. Maruhn, and W. Greiner, Phys. Rev. C **56**, 238 (1997).

[4] W. Q. Shen, J. Albinski, A. Gobbi, S. Gralla, K. D. Hildenbrand, N. Herrmann *et al.*, Phys. Rev. C **36**, 115 (1987).

[5] J. Toke, R. Bock, G. X. Dai, A. Gobbi, S. Gralla, K. D. Hildenbrand *et al.*, Nucl. Phys. **A440**, 327 (1985).

[6] M. G. Itkis, E. Vardaci, I. M. Itkis, G. N. Knyazheva, and E. M. Kozulin, Nucl. Phys. **A944**, 204 (2015).

[7] E. Vardaci, M. G. Itkis, I. M. Itkis, G. N. Knyazheva, and E. M. Kozulin, J. Phys. G: Nucl. Part. Phys. **46**, 103002 (2019).

[8] V. V. Volkov, Phys. Rep. **44**, 93 (1978).

[9] V. Zagrebaev and W. Greiner, J. Phys. G: Nucl. Part. Phys. **31**, 825 (2005).

[10] Y. Aritomo, K. Hagino, K. Nishio, and S. Chiba, Phys. Rev. C **85**, 044614 (2012).

[11] C. Simenel, Eur. Phys. J. A **48**, 152 (2012).

[12] G. G. Adamian, N. V. Antonenko, and W. Scheid, Nucl. Phys. **A678**, 24 (2000).

[13] A. K. Nasirov, G. Mandaglio, G. Giardina, A. Sobiczewski, and A. I. Muminov, Phys. Rev. C **84**, 044612 (2011).

[14] E. M. Kozulin, G. N. Knyazheva, I. M. Itkis, M. G. Itkis, A. A. Bogachev, L. Krupa *et al.*, Phys. Lett. B **686**, 227 (2010).

[15] I. M. Itkis, E. M. Kozulin, M. G. Itkis, G. N. Knyazheva, A. A. Bogachev, E. V. Chernysheva *et al.*, Phys. Rev. C **83**, 064613 (2011).

[16] E. M. Kozulin, G. N. Knyazheva, I. M. Itkis, M. G. Itkis, A. A. Bogachev, E. V. Chernysheva *et al.*, Phys. Rev. C **90**, 054608 (2014).

[17] E. M. Kozulin, G. N. Knyazheva, K. V. Novikov, I. M. Itkis, M. G. Itkis, S. N. Dmitriev, Y. S. Oganessian, A. A. Bogachev, N. I. Kozulina, I. Harca, W. H. Trzaska, and T. K. Ghosh, Phys. Rev. C **94**, 054613 (2016).

[18] E. M. Kozulin, G. N. Knyazheva, T. K. Ghosh, A. Sen, I. M. Itkis, M. G. Itkis *et al.*, Phys. Rev. C **99**, 014616 (2019).

[19] R. Bass, Nucl. Phys. **A231**, 45 (1974).

[20] R. du Rietz, E. Williams, D. J. Hinde, M. Dasgupta, M. Evers, C. J. Lin, D. H. Luong, C. Simenel, and A. Wakhle, Phys. Rev. C **88**, 054618 (2013).

[21] Y. T. Oganessian, V. K. Utyonkov, Y. V. Lobanov, F. S. Abdullin, A. N. Polyakov, R. N. Sagaidak *et al.*, Phys. Rev. C **79**, 024603 (2009).

[22] S. Hofmann, D. Ackermann, S. Antalic, V. F. Comas, S. Heinz, J. A. Heredia *et al.*, GSI Sci. Rep. **2008**, GSI Report 2009-1, 131 (GSI Helmholtzzentrum für Schwerionenforschung GmbH, 2009).

[23] S. Hofmann, S. Heinz, R. Mann, J. Maurer, G. Münzenberg, S. Antalic *et al.*, Eur. Phys. J. A **52**, 180 (2016).

[24] H. M. Albers, J. Khuyagbaatar, D. J. Hinde, I. P. Carter, K. J. Cook, M. Dasgupta *et al.*, Phys. Lett. B **808**, 135626 (2020).

[25] Proposal CERN Experiment IS550 P-344, http://cds.cern.ch/record/1482374/files/INTC-P-344.pdf.

[26] E. M. Kozulin, A. A. Bogachev, M. G. Itkis, I. M. Itkis, G. N. Knyazheva, N. A. Kondratiev *et al.*, Instrum. Exp. Tech. **51**, 44 (2008).

[27] D. J. Hinde, M. Dasgupta, J. R. Leigh, J. C. Mein, C. R. Morton, J. O. Newton, and H. Timmers, Phys. Rev. C **53**, 1290 (1996).

[28] S. Heinz, O. Beliuskina, V. Comas, H. M. Devaraja, C. Heinz, S. Hofmann *et al.*, Eur. Phys. J. A **51**, 140 (2015).

[29] E. V. Prokhorova, A. A. Bogachev, M. G. Itkis, I. M. Itkis, G. N. Knyazheva, N. A. Kondratiev *et al.*, Nucl. Phys. **A802**, 45 (2008).

[30] L. Corradi, A. M. Stefanini, C. J. Lin, S. Beghini, G. Montagnoli, F. Scarlassara, G. Pollarolo, and A. Winther, Phys. Rev. C **59**, 261 (1999).

[31] J. Wilczynski and H. W. Wilschut, Phys. Rev. C **39**, 2475 (1989).

[32] W. W. Wilcke, J. R. Birkelund, A. D. Hoover, J. R. Huizenga, W. U. Schröder, V. E. Viola, Jr., K. L. Wolf, and A. C. Mignerey, Phys. Rev. C **22**, 128 (1980).

[33] W. J. Swiatecki, Phys. Scr. **24**, 113 (1981).

[34] F. Gonnenwein, *The Nuclear Fission Process* (CRC, Boca Raton, FL, 1991), Chap. 8, p. 287.

[35] K. Nishio, S. Mitsuoka, I. Nishinaka, H. Makii, Y. Wakabayashi, H. Ikezoe, K. Hirose, T. Ohtsuki, Y. Aritomo, and S. Hofmann, Phys. Rev. C **86**, 034608 (2012).

[36] E. M. Kozulin, E. Vardaci, G. N. Knyazheva, A. A. Bogachev, S. N. Dmitriev, I. M. Itkis *et al.*, Phys. Rev. C **86**, 044611 (2012).

[37] V. E. Viola, K. Kwiatkowski, and M. Walker, Phys. Rev. C **31**, 1550 (1985).

[38] M. G. Itkis and A. Y. Rusanov, Phys. Part. Nucl. **29**, 160 (1998).

[39] M. G. Itkis, V. N. Okolovich, A. Y. Rusanov, and G. N. Smirenkin, Z. Phys. A: At. Nucl. **320**, 433 (1985).

[40] S. I. Mulgin, V. N. Okolovich, and S. V. Zhdanov, Phys. Lett. B **462**, 29 (1999).

[41] I. V. Pokrovsky, M. G. Itkis, J. M. Itkis, N. A. Kondratiev, E. M. Kozulin, E. V. Prokhorova *et al.*, Phys. Rev. C **62**, 014615 (2000).

[42] S. I. Mulgin, S. V. Zhdanov, N. A. Kondratiev, K. V. Kovalchuk, and A. Y. Rusanov, Nucl. Phys. **A824**, 1 (2009).

[43] V. Zagrebaev, Prog. Theor. Phys. Suppl. **146**, 642 (2002).

[44] V. I. Zagrebaev and W. Greiner, Nucl. Phys. **A944**, 257 (2015).

[45] M. K. Gaidarov, J. Phys.: Conf. Ser. **381**, 012112 (2012).

[46] C. Simenel, D. J. Hinde, R. du Rietz, M. Dasgupta, M. Evers, C. J. Lin, D. H. Luong, and A. Wakhle, Phys. Lett. B **710**, 607 (2012).